A Robust Adaptive Non-Singular Terminal Sliding Mode Control: Application to an Upper-Limb Exoskeleton with Disturbances and Uncertain Dynamics

Mouna Dali Hassen, Imen Laamiri, Nasreddine Bouguila

Laboratory of Automatic Signal and Image Processing, National School of Engineers of Monastir, University of Monastir, 5019, Tunisia

Corresponding author: mouna.dalihssan@gmail.com

This paper presents a new control strategy for uncertain upper-limb exoskeleton systems, which are known to have high nonlinearities, unmodeled dynamics, and uncertainties. The proposed technique is based on the terminal sliding mode control algorithm and its non-singular design method and incorporates an adaptive control approach to estimate the upper bounds of the unknown system uncertainties, which helps to improve the accuracy of the control and reduce the effects of disturbances. The stability of the proposed control strategy is confirmed using Lyapunov theory, and its effectiveness is tested on a two-degrees-of-freedom upper-limb exoskeleton. The results demonstrate that the proposed control scheme provides robust, fast, and finite-time convergence as well as an effective control approach capable of dealing with the disturbances and uncertainties that such systems are prone to.

KEYWORDS: exoskeletons, robustness, stability, sliding mode control, uncertain system.

1. Introduction

In recent years, the field of robotics and assistive technology has undergone a profound transformation, marked by remarkable advancements. Among these innovations, exoskeletons have emerged as a groundbreaking solution poised to enhance the quality of life for individuals living with mobility impairments. These wearable robotic devices are meticulously designed to augment the physical abilities of their users, offering a vast spectrum of applications that extend far beyond conventional boundaries. From aiding in medical rehabilitation to providing invaluable support in industrial contexts and military operations, exoskeletons hold the promise of transforming lives [3, 22].

Indeed, the study of exoskeletons has become a prominent focus of scientific research, driven by the ambition to unravel the intricacies of human physiology through the replication of its mechanisms, reflexes, and physical capabilities [16, 17]. Among the myriad functions these remarkable devices fulfil, the achievement of a stable and efficient walking cycle has emerged as a central area of investigation. Realizing a robotic walking cycle involves the pursuit of three fundamental objectives: ensuring unwavering stability, generating precise reference trajectories, and devising effective control strategies that optimize the desired trajectory.

At its core, an exoskeleton represents the epitome of the fusion between engineering ingenuity and human potential. These wearable marvels typically consist of a robust frame or structure, worn externally on the body, and are powered by motors or comparable mechanisms. These mechanisms are meticulously engineered to bestow augmented strength, endurance, and mobility upon the wearer [7, 23]. The applications of exoskeletons span a diverse array of fields, from their invaluable role in medical rehabilitation, where they enable individuals with mobility impairments to walk and engage in daily tasks, to their indispensable presence in industrial settings, where they empower workers to lift heavy objects and perform physically demanding tasks.

Yet, as we venture into the realm of robotic manipulators, a distinct and formidable challenge takes center stage, particularly in the domain of tracking control. This challenge has garnered increasing attention over the years, owing to the exigencies of achieving pinpoint accuracy in manipulating these multifaceted machines. The pursuit of flawless tracking hinges upon an intimate understanding of the dynamic characteristics that define these manipulators, a task rendered exceptionally challenging due to the highly interlinked, nonlinear, and ever-evolving nature of their dynamics [31]. Furthermore, the stakes are amplified in scenarios where robotic manipulators are deployed in tasks requiring a level of precision akin to welding, painting, and assembling, where even the most minor tracking errors can exert a deleterious influence on the final product's quality. As a result, researchers have fervently dedicated themselves to pioneering advanced control methodologies. These methodologies chart a course toward the attainment of impeccable tracking control, steadfastly navigating through the intricate labyrinth of complexities that shroud the dynamics of these manipulators [4, 5, 23-25, 27, 29].

The main contributions of this paper are listed as follows:

- A nonlinear uncertain exoskeleton system subjected to different forms of uncertainties and disturbances (dynamic parameter variations, friction losses, payload variation, external disturbances, and dynamic model uncertainties) is studied.
- An improved, robust NTSMC is established where the uncertainties affecting the system are assumed to be unknown, time-varying, yet norm-bounded. For this purpose, an adaptive law is constructed in order to estimate the upper limits of system uncertainties.
- Fast and finite-time convergence of the proposed control technique has been demonstrated for two-DOF upper-limb exoskeleton applications.

This paper is organized as follows: In Section 2, a literature review of related work is presented. Section 3 the robotic exoskeleton design and a reminder of its classical dynamic model are presented. The design of the adaptive non-singular terminal sliding mode control algorithm and its stability and robustness analysis are discussed in Section 4. Section 5 is devoted to the experimental validation of the proposed controller on a two-link upper-limb exoskeleton. Finally, the results and conclusions are drawn in Section 6.

2. Related Work

In the field of robotics and exoskeleton control, significant research efforts have been directed towards achieving precise control of wearable exoskeleton devices, particularly in contexts where user interaction and uncertainties play pivotal roles. This related work section provides an overview of relevant research endeavors and advanced control techniques.

Numerous advanced control strategies have been proposed to attain satisfactory tracking performance for robotic manipulators. These include backstepping control, adaptive control [4, 5, 16, 17, 29, 36], fuzzy control approach [15], neural network [18], and disturbance observers [13, 38], among others. Among the widely used techniques is sliding mode control (SMC), lauded for its design simplicity and robustness when dealing with dynamic uncertainty and disturbances [1-3]. SMC operates based on sliding surfaces, which are functions of the system states, and endeavors to maintain the system states on these surfaces, chosen to remain invariant over time. It has found application in linear and nonlinear systems across industries such as aerospace, automotive, electrical, and mechanical. SMC is renowned for its robustness against uncertainties and disturbances and its ability to achieve stable control systems with fast convergence [9, 26]. However, one of its drawbacks is the occurrence of high-frequency oscillations known as the "chattering phenomenon," which can result in suboptimal performance and increased wear on the system. Additionally, SMC ensures only asymptotic convergence to the desired state of the system and cannot compensate for variations in model parameters caused by human arm movements. Consequently, there is a need to develop more effective and advanced control techniques to address these limitations.

Various approaches have been explored to alleviate the high-frequency switching problem in sliding mode control systems. The authors in [10] opted for the saturation function (sat) instead of the signum function (sign), while the authors in [34, 36, 38] employed high-order sliding mode controllers, introduced non-ideal sliding surfaces, utilized smooth control inputs, and designed a boundary layer control law.

Terminal sliding mode control (TSMC) has been developed as a variation of the traditional SMC technique. It distinguishes itself by employing nonlinear switching hyperplanes to achieve finite-time convergence of the system's states, in contrast to SMC, which employs linear switching surfaces for asymptotic convergence of the system's states. TSMC utilizes a nonlinear switching hyperplane, termed the terminal sliding surface, designed to bring the system's states to the desired equilibrium point in finite time. The control law for TSMC is designed to drive the system's states to slide along the terminal sliding surface and converge to the desired equilibrium point within a finite time. TSMC offers the advantage of faster convergence of the system's states and improved robustness against disturbances and uncertainties. Studies on terminal sliding mode controllers applied to robotic manipulators have demonstrated their robustness and insensitivity to matched uncertainties [37]. Nevertheless, TSMC suffers from a singularity problem, prompting the development of fast terminal sliding mode control (FTSMC) as an extension of TSMC, which achieves higher convergence rates and stronger robustness despite significant initial system errors. FTSMC utilizes a modified terminal sliding surface that facilitates faster convergence of the system's states [34, 36, 37].

The conventional TSMC and FTSMC techniques involve control inputs that include negative fractional power terms, which may lead to infinite control inputs near the equilibrium point, creating the singularity problem. This issue can adversely affect the control system's performance and, in some cases, even damage the system. To address this challenge, non-singular terminal sliding mode control (NTSMC) has been proposed [6, 7, 10-12, 14, 20, 21, 28]. NTSMC modifies the control law used in TSMC to ensure the control input remains bounded near the equilibrium point, thereby eliminating the singularity problem and enhancing the control system's performance [8, 13]. NTSMC enables fast finite-time tracking control for practical devices and successfully eliminates the singularity problem present in conventional FTSMC techniques [33, 39]. It finds application in control systems for fast-moving systems, such as robots, aircraft, and automobiles, where rapid response times and dealing with significant initial system errors are critical [23-25, 27, 29].

In industrial and medical applications, exoskeleton devices interact closely with the user's body and the

external environment, leading to uncertainties within the systems. These uncertainties may arise from sensor noise, variations in the user's body mechanics, changes in the external environment, and limitations in the exoskeleton's design or control systems [10, 39]. Addressing these uncertainties is essential to ensure the performance and safety of the exoskeleton. Although various research studies have addressed non-linear systems with known uncertainties, real-world applications involve uncertainties arising from time-varying and unknown factors, making it challenging to determine their precise values in advance. Hence, techniques like adaptive control [4] or adaptive law with sliding mode control [19, 27, 28, 31, 38] are used to estimate these uncertainties.

In the work of Li and Huang [15], they outline a technique for designing MIMO adaptive fuzzy TSMC systems for robotic manipulators. This approach effectively mitigates chattering while preserving the benefits of traditional TSMC. It is specifically applied to address chattering in SMC and enhance its performance with respect to finite-time control. On the other hand, in the study by Mondal and Mahanta [25], they introduce an adaptive second-order TSM controller that effectively eliminates chattering when controlling robotic manipulators. Their approach involves employing an adaptive tuning method to handle uncertainties, even when the upper bounds of these uncertainties are unknown.

In this work, a robust adaptive non-singular terminal sliding mode controller is presented to effectively control the movements of an exoskeleton's wearer during activities, while considering system uncertainties and non-linearities to improve its dynamic performance.

3. System Description and Its Dynamic Model

3.1. System Description

An exoskeleton is a wearable device that can assist individuals with physical disabilities or provide additional support to workers engaged in physically demanding tasks. The exoskeleton typically includes a frame or structure that is worn externally and is powered by motors or other means to provide additional

strength, endurance, or mobility. It can be customized based on the user's needs, taking into account factors such as body size and shape, range of motion, and joint flexibility. The design of the exoskeleton must consider the kinematics and dynamics of the human body to ensure that it is a suitable and realistic solution for enhancing the user's physical abilities.

In this study, concern is given to an upper-limb orthosis performing shoulder and elbow movements connected by a revolute joint, as shown in Figure 1. This device uses a combination of mechanical, electrical, and control systems to amplify the movement of the wearer's arm, allowing them to perform a range of motions including extension, flexion, abduction, and adduction (Figure 2). They can help to improve the function of the affected limb, allowing the wearer to perform daily activities with greater ease and independence.

Figure 1
2 DOF upper-limb system configuration
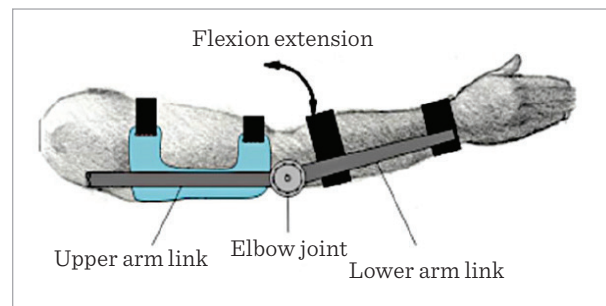
Figure 2
Movements of the human upper extremity
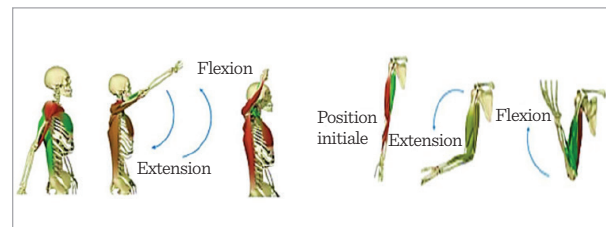
In Figure 3, the biomechanical model of the exoskeleton's upper limb is presented. It describes the structure of the human arm in relation to the exoskeleton. The model includes the actuated joints at the shoulder, elbow, and wrist, which are the focus of the study.

Figure 3
Mechanical model of the upper-limb exoskeleton in Solidworks
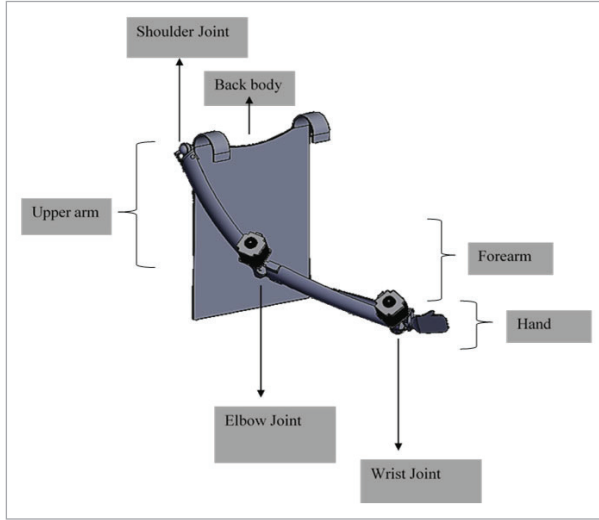
The prototype of the upper extremity system of the exoskeleton embodies a simplified rendition of the upper limb of the exoskeleton, intended for testing and refining the control law designed to enable the exoskeleton to track the wearer's movements.

3.2. Dynamic Model of the Upper-limb Orthosis

The dynamics of the upper-limb exoskeleton can be described by a set of nonlinear equations that take into account the various components of the system, such as the joints, actuators, and sensors, as follows:

$$\tau_{dyn} = \tau_{in} - \tau_f - \tau_{ext}, \tag{1}$$

where:

– $\tau_{dyn} \in \mathbb{R}^n$ is a vector of the dynamic forces due to inertial, centripetal, Coriolis, and gravitational effects.

$$\tau_{dyn} = M(q)\ddot{q} + C(q,\dot{q})\dot{q} + G(q), \tag{2}$$

where $M(q) \in \mathbb{R}^{n \times n}$ is the positive symmetric inertia matrix, $C(q, \dot{q}) \in \mathbb{R}^n$ relates to the Coriolis and centrifugal matrix, and $G(q) \in \mathbb{R}^n$ is the gravity vector of joint torques. $q \in \mathbb{R}^n$, $\dot{q} \in \mathbb{R}^n$ and $\ddot{q} \in \mathbb{R}^n$ refers respectively to the joint position vector, velocity vector and joint acceleration vector.

– τ_f is a vector of forces expressing friction losses.

In general, friction force is a function of Coulomb friction force and viscous friction force.

$$\tau_f = F_c sign(q) + F_v\, q, \tag{3}$$

where F_c is the diagonal matrix of the Coulomb friction forces, sign designates the sign function, and F_v is the diagonal matrix of the viscous friction coefficients.

– τ_{in} is the vector of the motor torque at the input of the transmission mechanism, defined on the motor side.

$$\tau_{in} = \tau - \tau_{off}. \tag{4}$$

The system is controlled by the input torque τ, which is the input torque of the gearbox, shifted by the amplifier offset τ_{off}

– τ_{ext} is the vector of bounded external forces applied to the exoskeleton and expressed in the joint space.

In the following, we state some assumptions that will be used later in the exoskeleton's stability analysis.

Assumption 1. We assume that the inertia matrix M(q) is invertible and has an upper bound defined by a positive constant: $\|M(q)\| < \beta_0$.

Assumption 2. The sum of Coriolis and centripetal torque vector and the gravity vector is enclosed by the following inequation:

$$\left\| C(q,\dot{q})\dot{q} + G(q) \right\| < \beta_1 + \beta_2 \|q\| + \beta_3 \left\| \dot{q} \right\|^2, \tag{5}$$

where β_1, β_2 and β_3 are positive numbers.

The dynamic model of the robotic exoskeleton is highly nonlinear, time-variant, and presents uncertainty from parameter variations, friction losses, and external disturbances and perturbations. Therefore, Equation (2) can be written as:

$$\tau_{dyn} = M_0(q)\ddot{q} + \Delta M(q) + C_0(q,\dot{q})\dot{q} + \Delta C(q,\dot{q}) + G_0(q) + \Delta G(q), \tag{6}$$

where $M_0(q)$, $C_0(q, q)$ and $G_0(q)$ are the nominal parts and while $\Delta M(q)$, $\Delta C(q, q)$ and $\Delta G(q)$ stand for uncertain parts in the dynamic model matrices.

Let τ_d be the lumped vector of input and external disturbances and non-modelled dynamics.

$$\tau_d(t) = -\Delta M(q) - \Delta C(q,\dot{q}) - \Delta G(q) - \tau_f - \tau_{off} - \tau_{ext}. \tag{7}$$

Therefore, (1) can be written in the form of the inverse dynamic model (IDM) that calculates the vector of input torque τ as a function of generalized coordinates of the exoskeleton in presence of friction, unknown interference and unmatched disturbances.

$$M_0(q)\ddot{q} + C_0(q,\dot{q})\dot{q} + G_0(q) = \tau + \tau_d(t) .\tag{8}$$

Assumption 3. Dynamic model uncertainty depends not only on external disturbances but also on the input signal. Therefore, if the acceleration signal is not involved in the control input, the lumped orthosis uncertainty will be enclosed by the following function relying on joints position and velocity such that:

$$\|\tau_d(t)\| < d_0 + d_1\|q\| + d_2\|\dot{q}\|^2 ,\tag{9}$$

where d_0, d_1 and d_2 are positive constants.

The inverse dynamic model (8) can be expressed in the following form:

$$\ddot{q} = M_0^{-1}(q)(\tau + \tau_d(t) - C_0(q,\dot{q})\dot{q} - G_0(q)) .\tag{10}$$

4. Control of the Exoskeleton Upper-limb

In this section, a robust non-singular terminal sliding mode (NTSM) technique is designed in the first part to control the exoskeleton's upper-limb movement. This technique can improve the system's performance by ensuring a stable and robust control system with fast convergence and singularity annulment. The algorithm can also provide improved robustness to system uncertainties and disturbances.

In the second part, a new robust adaptive non-singular terminal sliding mode (ANTSM) technique is developed by introducing a boundary layer around the sliding surface. This technique is based on the adaptive control and sliding mode approaches, and it is able to estimate the bounds of the uncertainties online and adjust the control input accordingly. This means that the control system can adapt to changes in the system dynamics, improving robustness, tracking performance, and chattering suppression in the presence of disturbances and uncertainties.

4.1. Robust Non Singular Terminal Sliding Mode Control (RNTSMC)

In this subsection, a robust NTSMC scheme is developed to avoid the TSMC technique's singularity problem.

We define q_d as the desired reference state of the exoskeleton to be reached so that the tracking error between the actual and desired trajectory and the tracking velocity error are expressed as follows:

$$\begin{cases} e = e_1 \\ e_1 = q - q_d \\ \dot{e} = e_2 = \dot{q} - \dot{q}_d \end{cases} .\tag{11}$$

Assumption 4. The dynamic model of the exoskeleton (8) can be expressed in the following form:

$$\ddot{q} = M_0^{-1}(q)(\tau - C_0(q,\dot{q})\dot{q} - G_0(q) + \tau_d) .\tag{12}$$

(10) can be formulated as follows:

$$\ddot{q} = M_0^{-1}(q)(-C_0(q,\dot{q})\dot{q} - G_0(q)) + M_0^{-1}(q)\tau + M_0^{-1}(q)d(t))$$
$$= f_0(q,\dot{q}) + M_0^{-1}(q)\tau + D(t)\tag{13}$$

where f_0 denotes the known bounded function as presented previously in Section 2.

$f_0(q,\dot{q}) = M_0^{-1}(q)(-C_0(q,\dot{q})\dot{q} - G_0(q))$ and $D(t) = M_0^{-1}(q)\tau_d(t)$.

By combining Equations (9) and (11), we get the following exoskeleton's nonlinear second order system:

$$\begin{cases} \dot{e}_1 = e_2 \\ \dot{e}_2 = f_0(q,\dot{q}) + M_0^{-1}(q)\tau + D(t) - \ddot{q}_d \end{cases} .\tag{14}$$

A non-singular terminal sliding (NTS) surface that ensures the convergence of the variable to the desired value in a finite time is introduced as:

$$S = e_1 + \beta|e_2|^{a/b} sign(e_2) .\tag{15}$$

where: $e_2 = \begin{bmatrix} e_{2_1} & \dots & \dots & e_{2_n} \end{bmatrix}^T$, $e_{2_i} = \dot{q}_i - \dot{q}_{id}$, q_d is the desired velocity trajectory;

$\beta = diag(\beta_1 \dots \beta_n)$ in which β is a positive constant; a and b are positive odd numbers satisfying $b < a < 2b$ [7, 10, 39];

$S(t) = \begin{bmatrix} s_1 & \dots & \dots & s_n \end{bmatrix}^T .$

When the sliding manifold S=0 is achieved, the actual position of the orthosis q_d attains the desired position q. Given the fact that:

$$sign(x) = \begin{bmatrix} sign(x_1) & .. & .. & sign(x_n) \end{bmatrix}^T$$
$$sign(x)^\gamma = \begin{bmatrix} |x_1|^{\gamma_1} sign(x_1) & .. & .. & |x_n|^{\gamma_n} sign(x_n) \end{bmatrix}^T \quad (16)$$

The NTS surface (15) can be rewritten:

$$S = e_1 + \beta sign(e_2)^{a/b}. \quad (17)$$

The time derivative of the NTS sliding surface S is then expressed as:

$$\dot{S} = e_2 + \beta \frac{a}{b} |e_2|^{a/b-1} \dot{e}_2 sign(e_2). \quad (18)$$

Substituting Equations (11) and (13) in Equation (18) results in:

$$\dot{S} = e_2 + \beta \frac{a}{b} |e_2|^{a/b-1} (f_0(q,\dot{q}) + M_0^{-1}(q)\tau + D(t) - \ddot{q}_d). \quad (19)$$

After selecting the sliding surface, one determines the control law that satisfies the terminal sliding condition. The control law applied to the orthosis is a sum of two control input functions, u_{eq} and u_n, where u_{eq} corresponds to the equivalent command proposed while u_n is designed to guarantee the convergence condition.

$$\tau = \tau_{eq} + \tau_n. \quad (20)$$

τ_{eq} corresponds to the reaching phase of the command with nonexistence of different forms of uncertainties ($D(t)$ =0) from $S = 0$:

$$\dot{S} = e_2 + \beta \frac{a}{b} |e_2|^{a/b-1} (f_0(q,\dot{q}) + M_0^{-1}(q)\tau + D(t) - \ddot{q}_d) = 0$$
$$\tau_{eq} = -\frac{1}{\beta} \frac{b}{a} |e_2|^{-a/b+1} M_0(q)e_2 + M_0(q)(-f_0(q,\dot{q}) + \ddot{q}_d) \quad (21)$$
$$= -\frac{1}{\beta} \frac{b}{a} |e_2|^{-a/b+1} M_0(q)e_2 + M_0(q)\ddot{q}_d + C_0(q,\dot{q})\dot{q} + G_0(q)$$

The discontinous command is defined by:

$$\tau_n = -Ksign(S), \quad (22)$$

where K is the gain chosen in order to ensure stability and sign is the signum function.

In fact, the use of the signum function in the high-frequency control term of SMC can lead to a chattering phenomenon characterized by rapid, small oscillations in the control input, which causes reduced control precision and stability issues. To overcome this problem, one can use an alternative expression, such as the "sat" function. The saturation function limits the magnitude of the sliding variable within a certain range, preventing the rapid oscillations caused by the signum function, such as:

$$\tau_n = -\frac{S}{\alpha_1 \|S\|} (\alpha_2(d_0 + d_1\|q\| + d_2\|\ddot{q}\|^2)). \quad (23)$$

Thus, according to Equations (17) and (21), the total terminal sliding mode command of the exoskeleton (18) can be written as follows:

$$\tau = -\frac{1}{\beta} \frac{b}{a} |e_2|^{-a/b+1} M_0(q)e_2 + M_0(q)\ddot{q}_d + C_0(q,\dot{q})\dot{q} + G_0(q).$$
$$.. - \frac{S}{\alpha_1 \|S\|} (\alpha_2(d_0 + d_1\|q\| + d_2\|\ddot{q}\|^2)) \quad (24)$$

Theorem 1. For the exoskeleton system (10) in which the lumped uncertainty fulfils the constraint (9) and suppose that the parameters d_0, d_1 and d_2 are unknown.

If the NTS surface is chosen as (18) and the global NTSMC control law is proposed as (24), then, the tracking error of the exoskeleton system converges to zero in finite time.

4.2. Adaptive Non Singular Terminal Sliding Mode Control(ANTSMC)

A robust ANTSMC scheme is developed in order to control the motion of the exoskeleton and track desired trajectories such as:

$$\tau_n = \begin{cases} -\dfrac{S}{\alpha_1 \|S\|} (\alpha_2(d_0 + d_1\|q\| + d_2\|\ddot{q}\|^2)) & if \ \|S\| \geq 0 \\ -\dfrac{S}{\alpha_1 \delta} (\alpha_2(d_0 + d_1\|q\| + d_2\|\ddot{q}\|^2)) & if \ \|S\| < 0 \end{cases} \quad (25)$$

The discontinuous control in Equation (23) will excite high-frequency dynamics. To address this issue, a new robust adaptive NTSMC technique can be used for tracking the exoskeleton upper-limb, where we replace the sign function with a boundary layer with a very small constant width δ (improving gain).

Based on the non-singular terminal sliding mode surface expression (15), we define the following control

law with the boundary layer concept to ensure fast tracking and solve the singularity problem:

$$\tau_n = \begin{cases} -\dfrac{S}{\alpha_1 \|S\|}(\alpha_2(d_0 + d_1\|q\| + d_2\|\dot{q}\|^2)) & if \ \|S\| \geq \delta \\[2mm] -\dfrac{S}{\alpha_1\delta}(\alpha_2(d_0 + d_1\|q\| + d_2\|\dot{q}\|^2)) & if \ \|S\| < \delta \end{cases} \quad (26)$$

The ANTSMC technique is based on the adaptive control approach, and it is able to estimate the bounds of the uncertainties online and adjust the control input accordingly. This means that the control system can adapt to changes in the system dynamics, providing improved robustness and tracking performance in the presence of disturbances and uncertainties.

$$\tau_n = \begin{cases} -\dfrac{S}{\alpha_1 \|S\|}(\alpha_2(\hat{d}_0 + \hat{d}_1\|q\| + \hat{d}_2\|\dot{q}\|^2)) & if \ \|S\| \geq \delta \\[2mm] -\dfrac{S}{\alpha_1\delta}(\alpha_2(\hat{d}_0 + \hat{d}_1\|q\| + \hat{d}_2\|\dot{q}\|^2)) & if \ \|S\| < \delta \end{cases} \quad (27)$$

The adaptive variables corresponding to d_0, d_1, d_2 in Equation (25) are $\hat{d}_0, \hat{d}_1, \hat{d}_2$,

where the adaptation law used for estimating the control law upper bound parameters is defined as:

$$\begin{cases} \dot{\hat{d}}_0 = \sigma_0 \|S\| \|M_0^{-1}\| \\[2mm] \dot{\hat{d}}_1 = \sigma_1 \|S\| \|M_0^{-1}\| \|q\| \\[2mm] \dot{\hat{d}}_2 = \sigma_2 \|S\| \|M_0^{-1}\| \|\dot{q}\|^2 \end{cases} \quad (28)$$

$\sigma_0, \sigma_1, \sigma_2$ are positive constants.

The adaptation errors are expressed as:

$$\begin{cases} \tilde{d}_0 = \hat{d}_0 - d_0 \\ \tilde{d}_1 = \hat{d}_1 - d_1 \\ \tilde{d}_2 = \hat{d}_2 - d_2 \end{cases} \quad (29)$$

Theorem 2. For the exoskeleton system (10) in which the lumped uncertainty fulfils the constraint (9), suppose that the parameters d_0, d_1 and d_2 are unknown.

If the NTS surface is chosen as (18) and the global adaptive NTSMC control law is developed as:

$$\tau = \begin{cases} \tau_{eq} - \dfrac{S}{\alpha_1 \|S\|}(\alpha_2(\hat{d}_0 + \hat{d}_1\|q\| + \hat{d}_2\|\dot{q}\|^2)) & if \ \|S\| \geq \delta \\[2mm] \tau_{eq} - \dfrac{S}{\alpha_1\delta}(\alpha_2(\hat{d}_0 + \hat{d}_1\|q\| + \hat{d}_2\|\dot{q}\|^2)) & if \ \|S\| < \delta \end{cases}, \quad (30)$$

where $\hat{d}_0, \hat{d}_1, \hat{d}_2$ are the estimates of d_0, d_1, d_2 respectively and updated with the adaptative law (28), then, the tracking error of the exoskeleton system converges to zero in finite time.

4.3. Stability Analysis

The nonlinear system faces uncertainties (7) with the control command (30) and based on the adaptive NTS surface (15) and the adaptation law (28) it can achieve the switching surface in a finite time.

Proof. To prove the stability of the considered system, we refer to the following Lyapunov function:

$$V = \frac{1}{2}S^2 + \frac{1}{2}\mu_0\tilde{d}_0^2 + \frac{1}{2}\mu_1\tilde{d}_1^2 + \frac{1}{2}\mu_2\tilde{d}_2^2. \quad (31)$$

The time derivative of Equation (31) gives:

$$\dot{V} = S\dot{S} + \mu_0\tilde{d}_0\dot{\tilde{d}}_0 + \mu_1\tilde{d}_1\dot{\tilde{d}}_1 + \mu_2\tilde{d}_2\dot{\tilde{d}}_2 \quad (32)$$

Substituting Equations (19) and (29) into Equation (32), we get:

$$\dot{V} = S(e_2 + \beta\frac{a}{b}|e_2|^{a/b-1}(f_0(q,\dot{q}) + M_0^{-1}(q)(\tau +) + D(t) - \ddot{q}_d)) + .. \\ ..\mu_0(\hat{d}_0 - d_0)\dot{\hat{d}}_0 + \mu_1(\hat{d}_1 - d_1)\dot{\hat{d}}_1 + \mu_2(\hat{d}_2 - d_2)\dot{\hat{d}}_2 \quad (33)$$

Replacing the adaptation law by its expression (28) in the latter equation, we obtain:

$$\dot{V} = S(e_2 + \beta\frac{a}{b}|e_2|^{a/b-1}(f_0(q,\dot{q}) + M_0^{-1}(q)\tau + D(t) - \ddot{q}_d)) + .. \\ ..\mu_0\sigma_0(\hat{d}_0 - d_0)\|S\|\|M_0^{-1}\| + .. \\ ..\mu_1\sigma_1(\hat{d}_1 - d_1)\|S\|\|M_0^{-1}\|\|q\| + \mu_2\sigma_2(\hat{d}_2 - d_2)\|S\|\|M_0^{-1}\|\|\dot{q}\|^2 \quad (34)$$

Inserting the expression of the control law (30) for $\|S\| \geq \delta$ into Equation (34) gives:

$$\dot{V} = S(e_2 + \beta\frac{a}{b}|e_2|^{a/b-1}(f_0(q,\dot{q}) + M_0^{-1}(q)(-\frac{1}{\beta}\frac{b}{a}|e_2|^{-a/b-1}M_0(q)e_2 + M_0(q)\ddot{q}_d \\ + C_0(q,\dot{q})\dot{q} + G_0(q) - \frac{S}{\alpha_1\|S\|}\alpha_2(\hat{d}_0 + \hat{d}_1\|q\| + \hat{d}_2\|\dot{q}\|^2)) + D(t) - \ddot{q}_d)) \\ + \mu_0\sigma_0(\hat{d}_0 - d_0)\|S\|\|M_0^{-1}\| + \mu_1\sigma_1(\hat{d}_1 - d_1)\|S\|\|M_0^{-1}\|\|q\| + \mu_2\sigma_2(\hat{d}_2 - d_2)\|S\|\|M_0^{-1}\|\|\dot{q}\|^2 \quad (35)$$

All the calculations are done; we get:

$$\dot{V} = -S(t)M_0^{-1}\frac{S}{\alpha_1\|S\|}\alpha_2(\hat{d}_0 + \hat{d}_1\|q\| + \hat{d}_2\|\dot{q}\|^2)) + S(t)D(t) + ..$$

$$..\mu_0\sigma_0(\hat{d}_0 - d_0)\|S\|\|M_0^{-1}\| + \mu_1\sigma_1(\hat{d}_1 - d_1)\|S\|\|M_0^{-1}\|\|q\| + ..$$

$$..\mu_2\sigma_2(\hat{d}_2 - d_2)\|S\|\|M_0^{-1}\|\|\dot{q}\|^2 \qquad (36)$$

$$\dot{V} \leq -\|M_0^{-1}\|\frac{S^2}{\alpha_1\|S\|}\alpha_2(d_0 + d_1\|q\| + d_2\|\dot{q}\|^2)) + \|S(t)\|\|D(t)\| + ..$$

$$..\mu_0\sigma_0\|(\hat{d}_0 - d_0)\|\|S\|\|M_0^{-1}\| + \mu_1\sigma_1\|(\hat{d}_1 - d_1)\|\|S\|\|M_0^{-1}\|\|q\| + ..$$

$$..\mu_2\sigma_2\|(\hat{d}_2 - d_2)\|\|S\|\|M_0^{-1}\|\|\dot{q}\|^2$$

$$\leq -\|M_0^{-1}\|\|S(t)\|(\frac{\alpha_2}{\alpha_1}(d_0 + d_1\|q\| + d_2\|\dot{q}\|^2 - \|D(t)\|) - ..$$

$$..\|(\hat{d}_0 - d_0)\|(\|S\| - \mu_0\sigma_0\|S\|\|M_0^{-1}\|) - \|(\hat{d}_1 - d_1)\|(\|S\| - \mu_1\sigma_1\|S\|\|M_0^{-1}\|)\|q\| - ..$$

$$..\|(\hat{d}_2 - d_2)\|(\|S\| - \mu_2\sigma_2\|S\|\|M_0^{-1}\|)\|\dot{q}\|^2 \qquad (37)$$

Let
$$\begin{cases} \rho_1 = \|M_0^{-1}\|(\frac{\alpha_2}{\alpha_1}(d_0 + d_1\|q\| + d_2\|\dot{q}\|^2 - \|D(t)\|)) \\ \rho_2 = (\|S\| - \mu_0\sigma_0\|S\|\|M_0^{-1}\|) \\ \rho_3 = (\|S\| - \mu_1\sigma_1\|S\|\|M_0^{-1}\|)\|q\| \\ \rho_4 = (\|S\| - \mu_2\sigma_2\|S\|\|M_0^{-1}\|)\|\dot{q}\|^2 \end{cases}$$

Equation (37) becomes:

$$\dot{V} \leq -\rho_1\sqrt{2}\frac{\|S\|}{\sqrt{2}} - \rho_2\sqrt{\frac{2}{\mu_0}}\|\tilde{d}_0\|\sqrt{\frac{\mu_0}{2}} - \rho_3\sqrt{\frac{2}{\mu_1}}\|\tilde{d}_1\|\sqrt{\frac{\mu_1}{2}} - \rho_4\sqrt{\frac{2}{\mu_2}}\|\tilde{d}_2\|\sqrt{\frac{\mu_2}{2}}. \qquad (38)$$

Then we get:

$$\dot{V} \leq -\min(\rho_1\sqrt{2}, \rho_2\sqrt{\frac{2}{\mu_0}}, \rho_3\sqrt{\frac{2}{\mu_1}}, \rho_4\sqrt{\frac{2}{\mu_2}}).(\frac{\|S\|}{\sqrt{2}} - \sqrt{\frac{\mu_0}{2}}\|\tilde{d}_0\| - \sqrt{\frac{\mu_1}{2}}\|\tilde{d}_1\| - \sqrt{\frac{\mu_2}{2}}\|\tilde{d}_2\|),$$

$$\dot{V} \leq -\rho''V^{1/2}(t) \qquad (39)$$

where $\rho'' = \min(\rho_1\sqrt{2}, \rho_2\sqrt{\frac{2}{\mu_0}}, \rho_3\sqrt{\frac{2}{\mu_1}}, \rho_4\sqrt{\frac{2}{\mu_2}})$.

The concerned system is stable if:

$$\begin{cases} \rho_1, \rho_2, \rho_3, \rho_4 > 0 \\ \mu_0\sigma_0\|M_0^{-1}\| < 1, \mu_1\sigma_1\|M_0^{-1}\| < 1, \mu_2\sigma_2\|M_0^{-1}\| < 1 \end{cases} \qquad (40)$$

According to the Lyapunov stability theory, it is sufficient to ensure that the derivative of Lyapunov function is negative.

Lemma 1: Consider $V(t)$, which is a continuous, positive-definite function that fulfils the differential inequation:

$$\dot{V}(x) + \lambda V^\eta(x) \leq 0, \qquad (41)$$

where $0 < \eta < 1$ and $\lambda > 0$.

Then the system ($\dot{x} = f(x)$) under the inequation (41) reaches the non-singular terminal sliding mode manifold and the tracking error converges to the equilibrium point within a finite time $t \leq \frac{V^{1/2}}{1/2}$.

The control scheme of the exoskeleton upper limb system using the robust adaptive non-singular terminal sliding mode in order to track the patient's various activities is presented in Figure 4.

Figure 4
The Control block of the orthosis
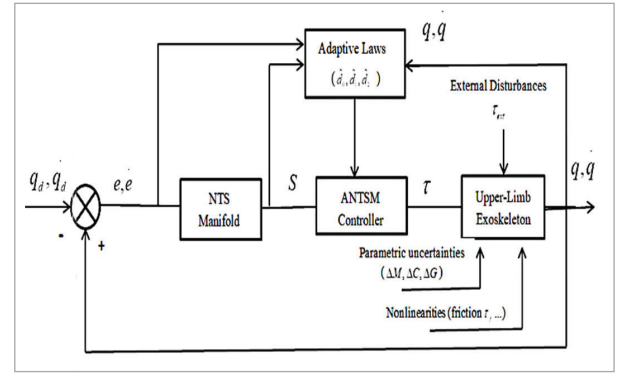
5. Simulation Results

The proposed controller efficiency is proved by simulating a two-link upper-limb orthosis whose configuration is presented in Figure 5.

The dynamic model of the simulated system under its matrix form is characterized by:

$$M(q)\ddot{q} + C(q,\dot{q})\dot{q} + G(q) = \tau + \tau_d(t), \qquad (42)$$

where:

$$q = \begin{pmatrix} q_1 \\ q_2 \end{pmatrix}, \tau = \begin{pmatrix} \tau_1 \\ \tau_2 \end{pmatrix}, G(q) = \begin{pmatrix} G_1 \\ G_2 \end{pmatrix}, \tau_d = \begin{pmatrix} \tau_{d_1} \\ \tau_{d_2} \end{pmatrix}$$

$$M(q) = \begin{pmatrix} M_{11} & M_{12} \\ M_{21} & M_{22} \end{pmatrix}, C(q) = \begin{pmatrix} C_{11} & C_{12} \\ C_{21} & C_{22} \end{pmatrix} \qquad (43)$$

Figure 5

Configuration of 2 DOF upper-limb exoskeleton
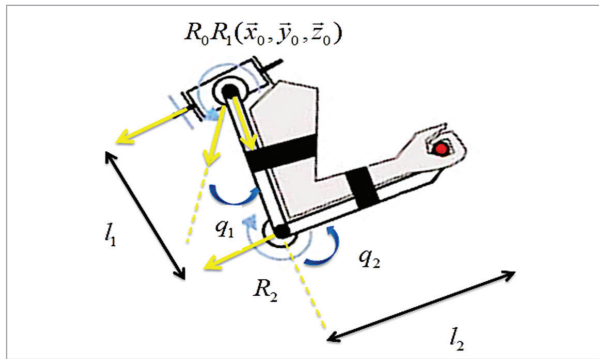
$$\begin{cases} M_{11} = (m_1 + m_2)L_1^2 + m_2L_2^2 + 2m_2L_1L_2cos(q_2) + J_1 \\ M_{12} = M_{12} = m_2L_2^2 + 2m_2L_1L_2cos(q_2) \\ M_{22} = m_2L_2^2 + J_2 \end{cases}$$

$$\begin{cases} C_{11} = -m_2L_1L_2sin(q_2)\dot{q}_1^2 - 2m_2L_1L_2sin(q_2)\dot{q}_1\dot{q}_2 \\ C_{12} = C_{21} = 0 \\ C_{22} = m_2L_1L_2sin(q_2)\dot{q}_2 \end{cases} \quad (44)$$

$$\begin{cases} G_1 = (m_1 + m_2)gL_1cos(q_1) + m_2gL_2cos(q_1 + q_2), \\ G_2 = m_2gL_2cos(q_1 + q_2) \end{cases}$$

where q1 and q_2 are the joint angles, q_1 and q_2 are the joint velocities, L_1 and L_2 are the arm joint lengths, m_1 and m_2 are the exoskeleton joint masses, J_1 and J_2 are the inertia of the upper-limb exoskeleton links1 and 2, g is the acceleration due to gravity.

The values of the exoskeleton nominal parameters used for simulation are grouped in Table 1.

Table 1

Simulation Parameters

Joint	1	2
Masses (m_1, m_2 [Kg])	0.4	1.2
Lengths (L_1, L_2 [m])	1	0.8
Inertia (J_1, J_2 [Kg.m²])	5	5
The acceleration of gravity (g [m/s²])	9.8	

The global time-varying disturbance and uncertainty vector is defined as:

$$\tau_d(t) = \begin{bmatrix} \tau_{d1}(t) \\ \tau_{d_2}(t) \end{bmatrix},$$

where:

$$\begin{cases} \tau_{d_1}(t) = 0.2\,sin(3t) + 0.02\,sin(26\pi t). \\ \tau_{d_2}(t) = 0.1\,sin(2t) + 0.01\,sin(26\pi t) \end{cases}$$

The initial state of the exoskeleton system is defined by the values of the joint positions and velocity introduced as:

$$\begin{bmatrix} q_1(0) \\ q_2(0) \end{bmatrix} = \begin{bmatrix} 0.8 \\ 0.9 \end{bmatrix}$$
$$\begin{bmatrix} \dot{q}_1(0) \\ \dot{q}_2(0) \end{bmatrix} = \begin{bmatrix} 0 \\ 0 \end{bmatrix}.$$

We consider a 10% variance in the nominal values of the exoskeleton joint masses when considering parameter uncertainty. $m_{1n} = 0.4kg, m_{2n} = 1.2kg$

The upper-limb orthosis is controlled to follow a desired movement trajectory, having the form of:

$$q_d = \begin{bmatrix} q_{1d} \\ q_{2d} \end{bmatrix} = \begin{bmatrix} q_{1d} = 1.25 - \dfrac{7}{5}exp(-t) + \dfrac{7}{20}exp(-4t) \\ q_{2d} = 1.4 - \dfrac{7}{5}exp(-t) + \dfrac{7}{20}exp(-4t) \end{bmatrix}.$$

Choosing the values of the controller parameters is an important task in the design and implementation of a control system.

Considering the ANTSMC scheme (30), the controller parameters are chosen to be:

b = 7, a = 5 $\beta = diag(\beta_1....\beta_n) = diag(2,2),\ \alpha_1 = 1, \alpha_2 = 1/2.$

Selected uncertainty bound parameters are: d_0, d_1, d_2= 2, 5, 9.

The constants of adaptive laws are: $\sigma_0 = \sigma_1 = \sigma_2 = 0.1$ and the initial adaptive parameters are selected as: $\hat{d}_0, \hat{d}_1, \hat{d}_2 = 0$.

To eliminate the chattering, the numerical simulation of the proposed control technique is performed with a boundary layer δ equal to 0.015.

5.1. RNTSMC Performance

Consider the robust non-singular terminal sliding mode control (RNTSMC) scheme developed in Subsection 3.1.

Figures 6-9 show the tracking performances of the upper limb exoskeleton when subjected to uncertainties and time-varying disturbances.

Figure 6
Position tracking performance of joint 1 and 2
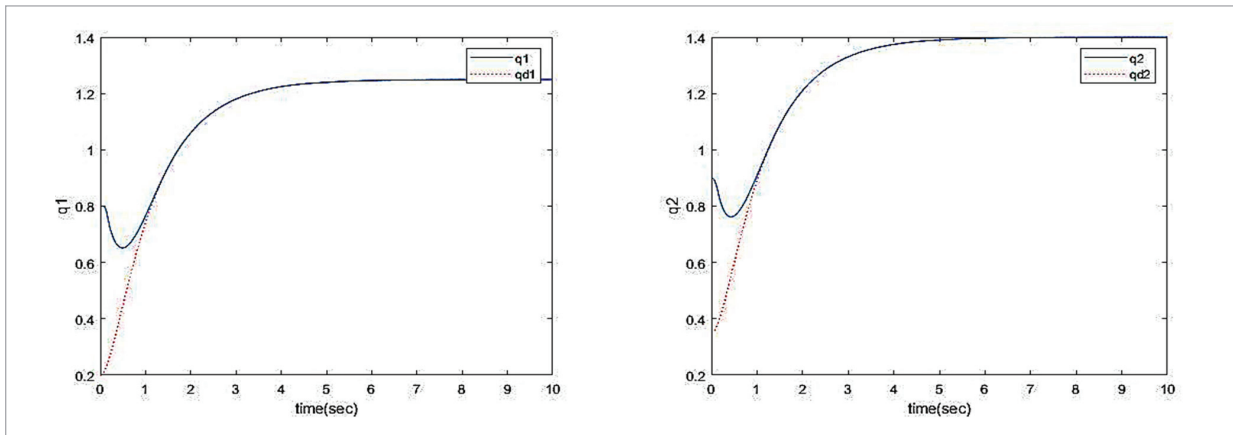
Figure 7
The tracking error of joint 1 and 2
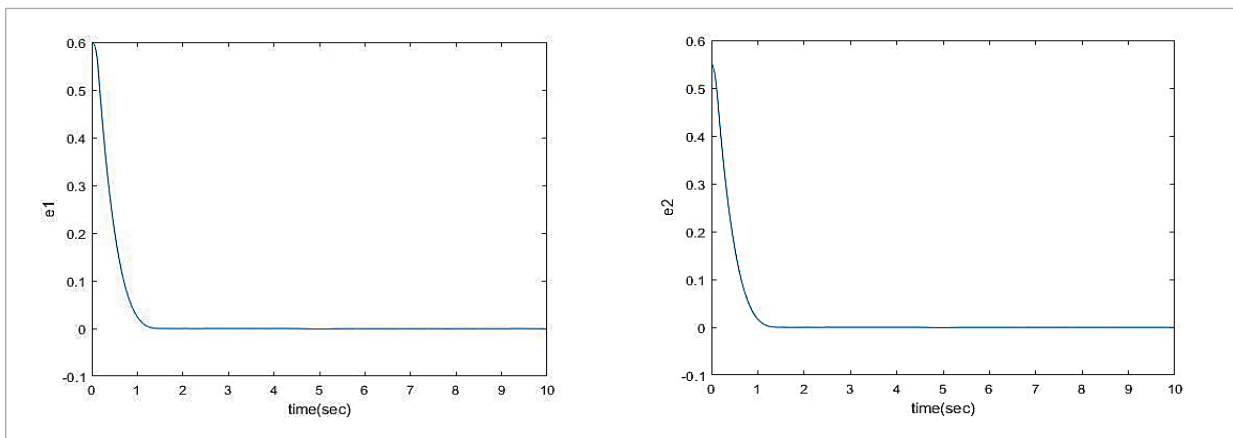
Figure 8
Velocity tracking performance of joint 1 and 2
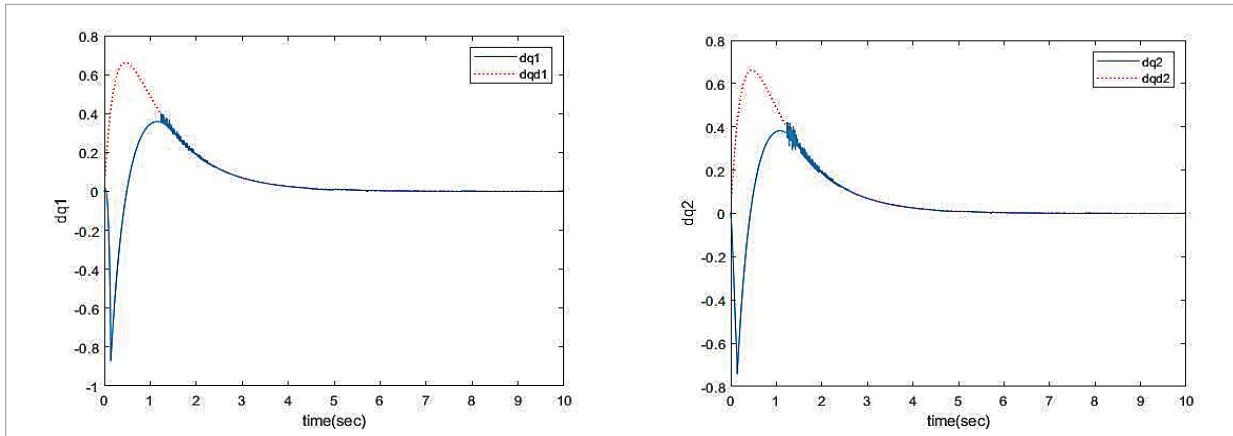
Figure 9
Sliding mode of joint 1 and 2
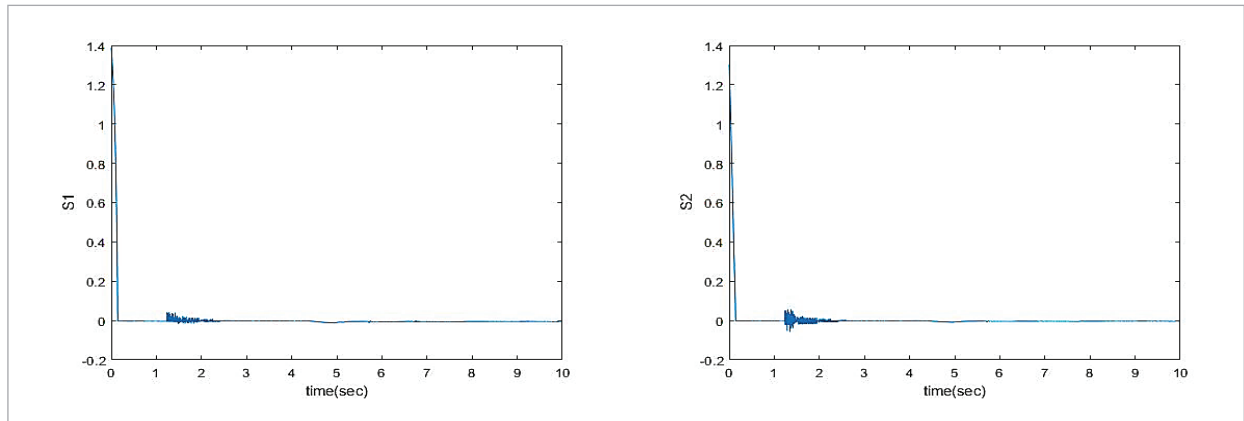
It can be seen that when this scheme is applied to an upper limb exoskeleton system, it can track the desired states and reach the reference states in a finite amount of time (approximately 1.3 seconds). The NTSMC strategy is able to force the tracking errors and the sliding surface to reach zero within a determined time, ensuring fast and accurate movement of the exoskeleton. However, as shown in Figures 8-9, the trajectory of the exoskeleton's joint velocities and sliding surfaces may present a negligible high-frequency commutation problem.

5.2. ANTSMC Performance

Consider the robust adaptive non-singular terminal sliding mode control (ANTSMC) scheme developed in Subsection 3. The tracking position and velocity of the exoskeleton's desired motion with the use of the proposed adaptive non-singular terminal sliding mode controller based on the boundary layer are given in Figures 10-11, respectively.

It can be observed that in this case, the joint velocity trajectories progress smoothly without the occurrence of the chattering phenomenon and without compromising their precision and robustness. As a result, the proposed adaptive non-singular terminal sliding mode controller based on the boundary layer control law can effectively track the desired trajectory of the upper-limb exoskeleton in finite time, compensate for system disturbances, ensure its robustness, and eliminate undesirable chattering effects.

Figure 10
Position tracking performance of joint 1 and 2
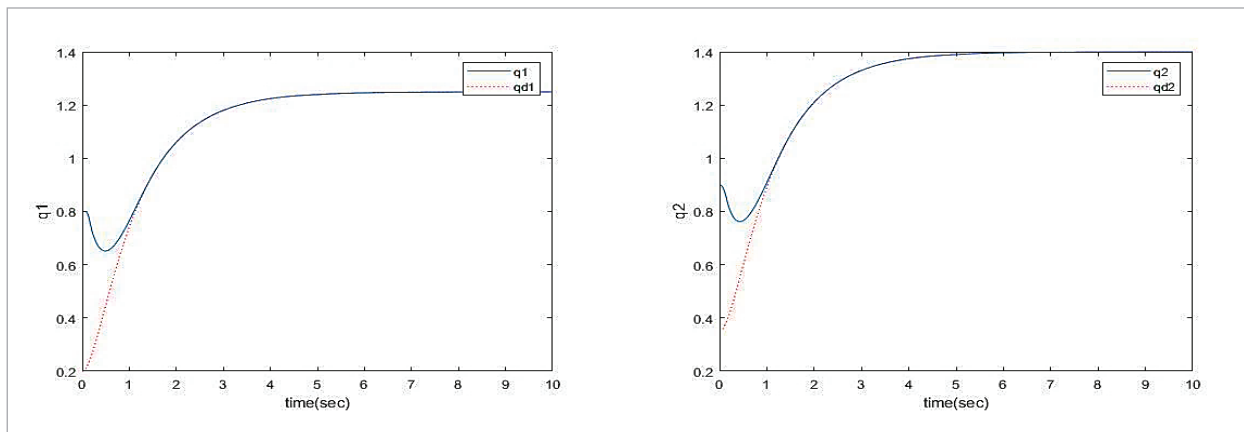
Figure 11

Velocity tracking performance of joint 1 and 2
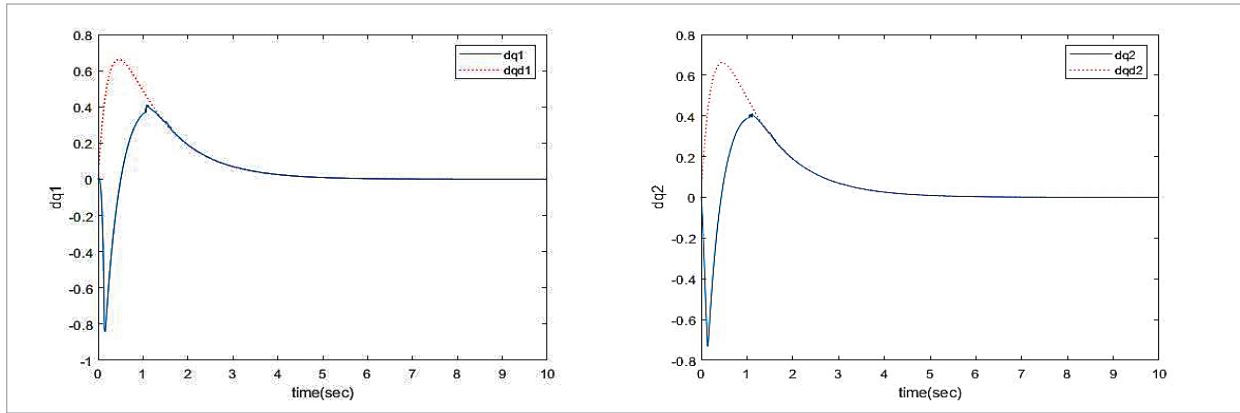
5.3. Comparison

To showcase the effectiveness of the proposed ANTSMC Control, a comparative analysis was conducted, pitting it against a recently developed sliding-mode controller. The specific control strategy being compared is adaptive super-twisting global nonlinear sliding-mode control, as presented by Mobayen et al. [24]. This analysis aims to highlight the advantages and distinctive features of ANTSMC Control in relation to the alternative sliding-mode controller.

Note that in order to make an accurate and reliable comparison of the different control schemes' performances, it is important to ensure that the simulations are implemented with the same system model under the same conditions, using the same set of system parameters, initial conditions, and disturbances listed in Section 4.

The details of the control algorithm designed by Mobayen et al. [24] are given as follows:

$$\tau = \tau_0 + \tau_1$$

$$\tau_0 = M_0(q)\ddot{q}_d + C_0(q,\dot{q})\dot{q} + G_0(q) - M_0(q)(\beta^{-1}\frac{b}{a}sign(e))^{2-a/b}$$

$$\tau_1 = -M_0(q)(K_1\tilde{s} + K_2 sign(\tilde{s})^\rho$$

$$\tilde{s} = e + \beta sign(e)^{a/b}$$

Table 2 presents the corresponding performance metrics, specifically the Integral of Absolute Error (IAE) and Integral of Squared Error (ISV). Figures 12-13 illustrate the position tracking error for the exoskeleton's joints 1 and 2 using the proposed ANTSM

Figure 12

Position tracking trajectories for Joint 1 under uncertainties and external disturbances of the developed ANTSMC and the controller designed by Mobayen et al.
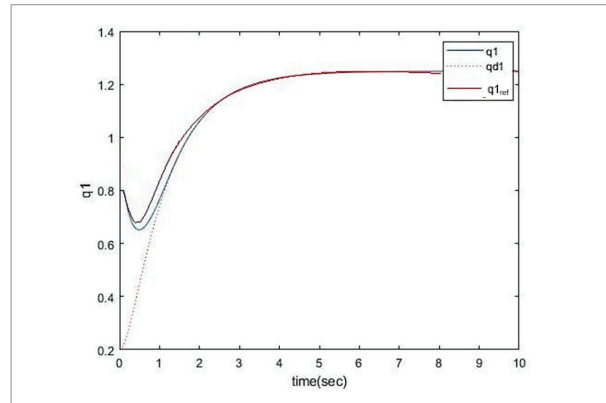
Figure 13

Position tracking trajectories for Joint 2 under uncertainties and external disturbances of the developed ANTSMC and the controller designed by Mobayen et al. [24]
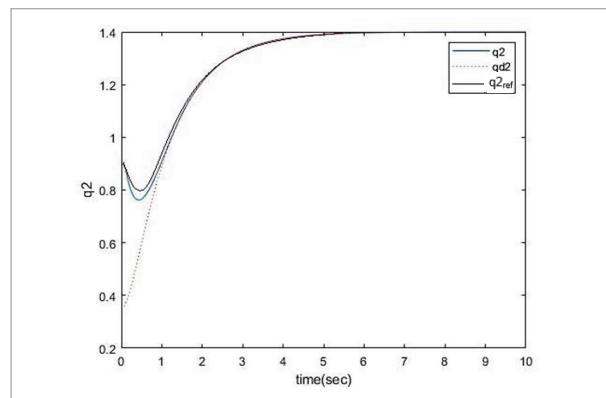
controller and the control scheme proposed by Mobayen et al. (TSMC) [24].

A quantitative analysis was conducted to evaluate the performance of the proposed ANTSMC approach in the presence of uncertainties and external disturbances. The analysis focused on two important metrics: Integral of Absolute Error (IAE) and Integral of Squared Value (ISV) as shown in Table 2.

Table 2
Comparative analysis

Controller	IAE		ISV	
	Joint1	Joint2	Joint1	Joint2
The proposed controller	0.5324	0.5186	0.2159	0.2846
Mobayen et al. [24]	0.6017	0.5725	0.2932	0.3057

It is evident that both control techniques guarantee the attainment of the desired exoskeleton motion within a finite timeframe and the convergence of the tracking error to zero. However, the proposed ANTSMC achieves a notably quicker transient response compared to the control algorithm devised by Mobayen et al. [24] when dealing with uncertainties and dynamic variations. The robust ANTSMC scheme achieves the fastest transients and the smallest settling time, resulting in the highest tracking precision. This means that the newly developed ANFTSM controller can quickly and precisely adjust the control inputs to achieve the desired state. The simulation results further support the superiority of the proposed scheme, as it outperforms other control methods in terms of achieving rapid and accurate tracking. This superiority is also confirmed by the quantitative analysis in Table 2, where the proposed scheme exhibits lower Integral of Absolute Error (IAE) values compared to the existing control method by Mobayen et al. [24].

In summary, the proposed ANTSMC demonstrates superior performance compared to conventional methods. It achieves a faster convergence rate, more precise tracking, reduced chattering, and improved robustness. Moreover, the control and adaptation technique employed in the developed adaptive approach eliminates the requirement of determining the upper bounds of uncertainties, which is a constraint typically encountered by conventional controllers.

6. Conclusion

The work presented in this paper addresses the control, stability, and robustness of a two-link upper-limb exoskeleton in the presence of various uncertainties and nonlinearities. These uncertainties include sensor noise, variations in the user's body mechanics, environmental changes, and limitations in the exoskeleton's design. To address these challenges, a robust adaptive non-singular terminal sliding mode control (ANTSMC) strategy with a boundary layer control law is proposed. The ANTSMC technique employs an adaptive control approach to estimate the uncertainties online and adjust the control input accordingly. This allows the control system to adapt to changes in the system dynamics, ensuring fast and finite-time convergence while improving tracking performance with a smooth and chatterless control signal, even in the presence of disturbances and uncertainties. However, Real-world testing with a robotic exoskeleton is crucial to validate the technique, assess performance, identify limitations, and improve it. Future research should focus on experimental studies to evaluate practicality, address challenges, and enhance reliability, contributing to advanced upper-limb rehabilitation exoskeleton systems.

References

1. Abdallah, C., Dawson, D., Dortao, P., Jamshidi, M. Survey of Robust Control for Rigid Robots. IEEE Control Systems Magazine, 1991, 11(2), 24-30. https://doi.org/10.1109/37.67672

2. Bartolini, G., Pisano, A., Punta, E. A Survey of Applications of Second-Order Sliding Mode Control to Mechanical Systems. International Journal of Control, 2003, 76 (9/10), 875-892. https://doi.org/10.1080/0020717031000099010

3. Bembli, S., ep Haddad, N. K., Belghith, S. Stability Study and Robustness Analysis of an Exoskeleton-Upper Limb System. 18th International Multi-Conference on Systems, Signals & Devices, 2021. https://doi.org/10.1109/SSD52085.2021.9429352

4. Benamor, A., Messaoud, H. Robust Adaptive Sliding Mode Control for Uncertain Systems with Unknown Time-Varying Delay Input. ISA Transactions, 2018, 79, 1-12. https://doi.org/10.1016/j.isatra.2018.04.017

5. Bkekri, R., Benamor, A., Alouane, M. A., Fried, G., Messaoud, H. Robust Adaptive Sliding Mode Control for a Human-Driven Knee Joint Orthosis. Industrial Robot: An International Journal, 2018, 45(3), 379-389. https://doi.org/10.1108/IR-11-2017-0205

6. Boukattaya, M., Gassara, H. Time-Varying Nonsingular Terminal Sliding Mode Control for Uncertain Second-Order Nonlinear Systems with Prespecified Time. International Journal of Adaptive Control and Signal Processing, 2022, 2017-2040. https://doi.org/10.1002/acs.3445

7. Corradini, M.L., Cristofaro, A. Nonsingular Terminal Sliding-Mode Control of Nonlinear Planar Systems with Global Fixed-Time Stability Guarantees. Automatica, 95, 561-565. https://doi.org/10.1016/j.automatica.2018.06.032

8. Cruz-Ortiz, D., Chairez, I., Poznyak, A. Non-Singular Terminal Sliding-Mode Control for a Manipulator Robot Using a Barrier Lyapunov Function. ISA Trans, 2022, 121, 268-283. https://doi.org/10.1016/j.isatra.2021.04.001

9. Cui, N., Wang, B., Mao, N. Terminal Sliding Mode Control Method for Robotic Manipulators. Aerospace Control, 2018, 173 (3), 34-40.

10. Feng, Y., Han, F., Yu, X., Stonier, D., Man, Z. Tracking Precision Analysis of Terminal Sliding Mode Control Systems with Saturation Functions. Advances in Variable Structure Systems, 2000. https://doi.org/10.1142/9789812792082_0030

11. Ghrab, S., Benamor, A., Messaoud, H. A New Robust Discrete-Time Sliding Mode Control Design for Systems with Time-Varying Delays on State and Input and Unknown Unmatched Parameter Uncertainties. Mathematics and Computers in Simulation, 2021, 190, 921-945. https://doi.org/10.1016/j.matcom.2021.06.009

12. Gong, W., Li, B., Yang, Y., Ban, H., Xiao, B. Fixed-Time Integral-Type Sliding Mode Control for the Quadrotor UAV Attitude Stabilization Under Actuator Failures. Aerospace Science and Technology, 2019, 95, 105444. https://doi.org/10.1016/j.ast.2019.105444

13. Han, J.Q., Wu, A.G., Dong, N. Terminal Sliding Mode Control for Robotic Manipulator Based on Sliding Mode Disturbance Observer. Journal of Central South University (Science and Technology), 2020, 51(10), 2749-2757.

14. Hassen, M. D., Laamiri, I. and Messaoud, H. Exoskeleton Dynamic Modeling and Identification with Load and Temperature-Dependent Friction Model, IEEE 2nd International Conference on Signal, Control and Communication (SCC), 2021, 14-19. https://doi.org/10.1109/SCC53769.2021.9768354

15. Huang, Y. C., Li, T.-H. S. Fuzzy Terminal Sliding-Mode Controller for Robotic Manipulators. IEEE International Conference on Mechatronics, 2005.

16. Kang, H.-B., Wang, J.-H. Adaptive Control of 5 DOF Upper-Limb Exoskeleton Robot with Improved Safety. ISA Transactions, 2013, 52(6), 844-852. https://doi.org/10.1016/j.isatra.2013.05.003

17. Khan, A.M., Yun, D., Ali, M. A., Zuhaib, K. M., Yuan, C., Iqbal, J., Han, J., Shin, K., Han, C. Passivity Based Adaptive Control for Upper Extremity Assist Exoskeleton. International Journal of Control, Automation and Systems, 2016, 14(1), 291-300. https://doi.org/10.1007/s12555-014-0250-x

18. Kumar, N., Panwar, V., Sukavanam, N., Sharma, S. P., Borm, J. H. Neural Network-Based Nonlinear Tracking Control of Kinematically Redundant Robot Manipulators. Mathematical and Computer Modelling, 2011, 53(9-10). https://doi.org/10.1016/j.mcm.2011.01.014

19. Labbadi, M., Cherkaoui, M. Robust Adaptive Nonsingular Fast Terminal Sliding-Mode Tracking Control for an Uncertain Quadrotor UAV Subjected to Disturbances. ISA Trans, 2020, 99, 290-304. https://doi.org/10.1016/j.isatra.2019.10.012

20. Li, Z., Zhai, J., Karimi, H. R. Adaptive Finite Time Super Twisting Sliding Mode Control for Robotic Manipulators with Control Backlash. International Journal of Robust and Nonlinear Control, 2021. https://doi.org/10.1002/rnc.5744

21. Liang, X., Wan, Y., Zhang, C. Task Space Trajectory Tracking Control of Robot Manipulators with Uncertain Kinematics and Dynamics. Mathematical Problems in Engineering, 2017, 1-19. https://doi.org/10.1155/2017/4275201

22. Liu, H., Tao, J., Lyu, P. Human-Robot Cooperative Control Based on sEMG for the Upper Limb Exoskeleton Robot. Robotics and Autonomous Systems, 2019. https://doi.org/10.1016/j.robot.2019.103350

23. Madani, T., Daachi, B., Djouani, K. Non-Singular Terminal Sliding Mode Controller: Application to an Actuated Exoskeleton. Mechatronics, 2016, 33, 136-145. https://doi.org/10.1016/j.mechatronics.2015.10.012

24. Mobayen, S., Tchier, F., Ragoub, L. Design of an Adaptive Tracker for N-Link Rigid Robotic Manipulators

Based on Super-Twisting Global Nonlinear Sliding Mode Control. International Journal of Systems Science, 2017, 48(9), 1990-2002. https://doi.org/10.1080/00207721.2017.1299812

25. Mondal, S., Mahanta, C. Adaptive Second Order Terminal Sliding Mode Controller for Robotic Manipulators. Journal of the Franklin Institute, 2014, 351(4), 2356-2377. https://doi.org/10.1016/j.jfranklin.2013.08.027

26. Mu, C., He, H. Dynamic Behavior of Terminal Sliding Mode Control. IEEE Transactions on Industrial Electronics, 2018, 65(4), 3480-3490. https://doi.org/10.1109/TIE.2017.2764842

27. Plestan, F., Shtessel, Y., Bregeault, V., Poznyak, A. New Methodologies for Adaptive Sliding Mode Control. International Journal of Control, 2010, 83(9), 1907-1919. https://doi.org/10.1080/00207179.2010.501385

28. Qiao, L., Zhang, W. Trajectory Tracking Control of AUVs via Adaptive Fast Nonsingular Integral Terminal Sliding Mode Control. IEEE Transactions on Industrial Informatics, 2020, 16, 1248-1258. https://doi.org/10.1109/TII.2019.2949007

29. Riani, A., Madani, T., Benallegue, A., Djouani, K. Adaptive Integral Terminal Sliding Mode Control for Upper-Limb Rehabilitation Exoskeleton. Control Engineering Practice, 2018, 75, 108-117. https://doi.org/10.1016/j.conengprac.2018.02.013

30. Roula, N., Chemori, A., Rizk, R., Zaatar, Y. On Control Design for a Lower Limb Orthosis: A Comparative Study in Different Operating Conditions. Mechanisms and Machine Science, 2018, 81-97. https://doi.org/10.1007/978-3-319-89911-4_7

31. Wang, C., Wen, G., Peng, Z., Zhang, X. Integral Sliding-Mode Fixed-Time Consensus Tracking for Second-Order Non-Linear and Time Delay Multi-Agent Systems. Journal of the Franklin Institute, 2019, 356, 3692-3710. https://doi.org/10.1016/j.jfranklin.2019.01.047

32. Wang, X., Li, S. Finite-Time Trajectory Tracking Control of Underactuated Autonomous Surface Vessels Based on Non-Singular Terminal Sliding Mode. Australian Journal of Electrical and Electronics Engineering, 2012, 9(3), 235-246. https://doi.org/10.1080/1448837X.2012.11464328

33. Wang, Y.Y., Chen, J.W., Yan, F., Zhu, K.W., Chen, B. Adaptive Super-Twisting Fractional-Order Nonsingular Terminal Sliding Mode Control of Cable-Driven Manipulators. ISA Transactions, 2019, 86, 163-180. https://doi.org/10.1016/j.isatra.2018.11.009

34. Wang, Y., Chen, M., Song, Yu. Terminal Sliding-Mode Control of Uncertain Robotic Manipulator System with Predefined Convergence Time. Complexity, 2021. https://doi.org/10.1155/2021/9991989

35. Wu, Y., Wang, L., Zhang, J., Li, F. Path Following Control of Autonomous Ground Vehicle Based on Nonsingular Terminal Sliding Mode and Active Disturbance Rejection Control, IEEE Transactions on Vehicular Technology, 2019, 68(7), 6379-6390. https://doi.org/10.1109/TVT.2019.2916982

36. Yi, S., Zhai, J. Adaptive Second-Order Fast Nonsingular Terminal Sliding Mode Control for Robotic Manipulators. ISA Transactions, 2019, 90, 41-51. https://doi.org/10.1016/j.isatra.2018.12.046

37. Yu, S., Yu, X., Shirinzadeh, B., Man, Z. Continuous Finite-Time Control for Robotic Manipulators with Terminal Sliding Mode, Automatica, 2005, 41(11), 1957-1964. https://doi.org/10.1016/j.automatica.2005.07.001

38. Zheng, W., Chen, M. Tracking Control of Manipulator Based on High-Order Disturbance Observer. IEEE Access, 2018, 6, 26753-26764. https://doi.org/10.1109/ACCESS.2018.2834978

39. Zhu, Y., Wu, D., Li, S. Non-Singular Fast Terminal Sliding Mode Tracking Control of a 2-DOF Robotic Manipulator Using Finite-Time Extended State Observer. In Proceedings of the 2021 33rd Chinese Control and Decision Conference (CCDC), Kunming, China, 22-24 May 2021; IEEE: Piscataway, NJ, USA. https://doi.org/10.1109/CCDC52312.2021.9601551